are recorded in Table I (column 4). The universality of the $(\partial \ln \epsilon/\partial P)_{T,n's}$ value at 25 °C was next checked by evaluating ϕ_V at 25 °C for barium chloride and calcium chloride, the necessary data for both of which are available.[4,29-31] The calculated and the experimental ϕ_V values (for $C = 5 \times 10^{-4}$ to 0.3 M) again are in good agreement (Table I, column 4). However, for $C > 0.3$ M the agreement between the calculated and the experimental ϕ_V values is not so good and it affected the overall $\sigma_\phi{}^2$ ($C = 5 \times 10^{-4}$ to 1 M) (Table I, column 5). This failure may be due either to (1) evaluation of $(\partial \ln \epsilon/\partial P)_{25°C,p=1atm,n's}$ in the manner suggested above or to (2) the assumption that $(\partial B/\partial P) = 0$. It was, however, observed that if $(\partial \ln \epsilon/\partial P)_{25°C,P=1atm,n's}$ has the value 88.84×10^{-6} bar^{-1}, the overall agreement between the observed and the calculated ϕ_V values is improved somewhat but it would yield 2.993 and 15.55 as the limiting slope for the ϕ_V data of 1:1 and 2:1 electrolytes. These slopes are evidently not consistent with the experimental[19,20,28] and theoretical values.[17] The probable failure for $C > 0.3$ M may therefore lie with the assumption that $(\partial B/\partial P) = 0$. Since $(\partial B/\partial P)$ is a quantity characteristic of an electrolyte and as it involves additional contributions to ϕ_V according to a theory[1,2] which is applicable to concentrated solutions, we evaluated it by fitting the observed ϕ_V data for 1 M solution to eq 24. This value of $\partial B/\partial P$ was next used to calculate ϕ_V values for the electrolyte at all concentrations from expression 24. The agreement between the observed and the calculated ϕ_V values at 25 °C has now improved considerably (Table I, column 6).

The $(\partial \ln \epsilon/\partial P)_{25°C,P=1atm,n's}$ value of 60.66×10^{-6} bar^{-1} obtained from our analysis of ϕ_V data is greater than the recent value[13] of 47.10×10^{-6} bar^{-1} but is less than the value 76×10^{-6} bar^{-1} which Bahe and Jung[8] obtained from their analysis of ϕ_V data in terms of their lattice model.[1,2] Nevertheless, in view of Bahe and Jung's observations,[8] our value of $[\partial \ln \epsilon/\partial P]$ at 25 °C and at 1 atm does not seem impossible.

Acknowledgments. The patience of Professor L. G. Hepler, with whom many valuable discussions were held, is gratefully acknowledged. The author thanks the authorities of the Panjab Agricultural University, Ludhiana, India, for a leave of absence. This work was supported by the National Research Council of Canada.

References and Notes

(1) L. W. Bahe, *J. Phys. Chem.*, **76**, 1062 (1972).
(2) L. W. Bahe and D. Parker, *J. Am. Chem. Soc.*, **97**, 5664 (1975).
(3) M. H. Lietzke, R. W. Stoughton, and R. M. Fuoss, *Proc. Natl. Acad. Sci. U.S.A.*, **58**, 39 (1968).
(4) P. P. Singh, *J. Am. Chem. Soc.*, **99**, 1312 (1977).
(5) H. G. Hertz, R. Tutsch, and N. S. Bowman, *J. Phys. Chem.*, **80**, 417 (1976).
(6) M. S. Goldenberg, P. Kruss, and S. K. F. Luk, *Can. J. Chem.*, **53**, 1007 (1975).
(7) H. S. Harned and B. B. Owen in "The Physical Chemistry of Electrolytic Solutions", 3rd ed, Reinhold, New York, N.Y., 1967, p 79.
(8) L. W. Bahe and K. A. Jung, *Can. J. Chem.*, **54**, 824 (1976).
(9) Reference 5, pp 524–525.
(10) D. D. Masson, *Philos. Mag.*, **8**, 218 (1929).
(11) Reference 5, pp 359, 361.
(12) O. Redlich, *J. Phys. Chem.*, **44**, 619 (1940).
(13) B. B. Owen, R. C. Miller, C. E. Milner, and H. L. Cogan, *J. Phys. Chem.*, **65**, 2065 (1961).
(14) F. E. Harris, E. W. Haycock, and B. J. Alder, *J. Phys. Chem.*, **57**, 978 (1953).
(15) A. Falkenberg, *Ann. Phys. (Leipzig)*, **61**, 145 (1920).
(16) S. Kyropoulos, *Z. Phys.*, **40**, 507 (1926).
(17) O. Redlich and D. Meyer, *Chem. Rev.*, **64**, 221 (1964).
(18) O. Redlich and J. Bigeleisen, *J. Am. Chem. Soc.*, **64**, 760 (1942).
(19) L. G. Hepler, J. M. Stokes, and R. H. Stokes, *Trans. Faraday Soc.*, **61**, 20 (1965).
(20) L. A. Dunn, *Trans. Faraday Soc.*, **65**, 1898 (1968).
(21) R. C. Weast, Ed., "Handbook of Chemistry and Physics", 49th ed, Chemical Rubber Publishing Co., Cleveland, Ohio, 1968, p F-S.
(22) Reference 5, p 362, 363.
(23) Reference 5, pp 361, 725.
(24) F. Vaslow, *J. Phys. Chem.*, **70**, 2286 (1966).
(25) F. Vaslow, *J. Phys. Chem.*, **73**, 3745 (1969).
(26) A. F. Scott, *J. Phys. Chem.*, **35**, 2315 (1931).
(27) T. F. Young and M. B. Smith, *J. Phys. Chem.*, **58**, 716 (1954).
(28) J. L. Fortier, P. A. Leduc, and J. E. Desnoyers, *J. Solution Chem.*, **3**, 323 (1974).
(29) L. A. Dunn, *Trans. Faraday Soc.*, **62**, 2348 (1966).
(30) A. Perron, J. E. Desnoyers, and F. J. Millero, *Can. J. Chem.*, **52**, 3738 (1974).
(31) Reference 5, p 361.

Photocurrent Spectroscopy of Semiconductor Electrodes in Liquid Junction Solar Cells

A. Heller,* K.-C. Chang, and B. Miller

Contribution from the Bell Laboratories, Murray Hill, New Jersey 07974.
Received June 16, 1977

Abstract: Photocurrent spectra obtained by a two-beam (one pump-one probe) spectroscopic method on the semiconductor electrode of liquid junction solar cells can vary with the pump irradiance. In cells with n-type CdS, CdSe, CdTe, and GaAs photoanodes and chalogenide anion solutions this irradiance dependence results from and sensitively detects the presence of carrier recombination centers. With semiconductors showing no detectable recombination centers by this technique, cells with external solar to electrical conversion efficiences of 8–9% have been made. Classical single beam photocurrent spectroscopy reveals that poor short-wavelength response in semiconductor liquid junction solar cells is due to surface or near surface recombination centers and resembles p–n junction solar cells in this respect. Lowered long-wavelength response is associated with shrinkage of the depletion region of imperfect and overdoped semiconductors.

Introduction

The analysis of efficiency losses in photovoltaic solar cells requires the identification of carrier recombination centers and other mechanisms leading to photocurrent decrease.[1] Photocurrent spectra for semiconductor–liquid junction cells[2] have been used to determine band gaps and redox solution absorbance[2,3] but also contain many other features which relate directly to cell operation such as short- and long-wavelength defects and dependence on incident light intensity. This latter dependence may account for cell efficiency deterioration observed by others at light levels corresponding to only 0.01–0.1 of typical solar irradiance.[3,4]

We have recently introduced a method of two-beam spec-

0002-7863/78/1500-0684$01.00/0

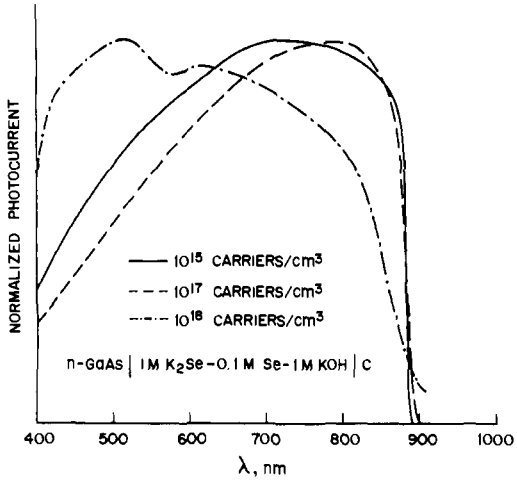

Figure 1. Effect of the doping level on the photocurrent spectra of n-GaAs|1 M K_2Se-0.1 M Se-1 M KOH|C solar cells.

troscopy of the semiconductor electrode[5] whose implications for photovoltaics we extend in this paper, in combination with additional results in classical single-beam photocurrent spectroscopy. We will discuss the origin of short- and long-wavelength defects, transitions to or from states within the forbidden band, and the intensity dependence, and correlate these results of one- and two-beam methods with the performance of semiconductor-liquid junction solar cells.

Results and Discussion

The photocurrent spectrum of an ideal semiconductor liquid junction solar cell, after correction for solution absorption losses (and for the spectrum of the light source), is flat at wavelengths below the edge and is independent of irradiance up to well above solar levels. We shall consider examples of and causes for deviations from the ideal behavior.

Long-Wavelength Defects. Spectra with long-wavelength defects show reduced photocurrent response near the band gap. Figure 1 shows the development of a long-wavelength defect in the n-GaAs|1 M K_2Se-0.1 M Se-1 M KOH|C cell which becomes severe when the (Sn) doping reaches 10^{18} carriers/cm^3. The spectra are corrected for the number of incident photons and the relative response is normalized to bring the maxima of the curves to unity. The actual integrated quantum efficiency is not substantially different for cells made with 10^{15} and 10^{17} carriers/cm^3 crystals (~65%) but is fourfold lower (~15%) at 2×10^{18} carriers/cm^3. This indicates that there is no enhancement of the short-wavelength response, but rather a drastic loss above ~600 nm.

Causes for long-wavelength defects are the following. Photons near the band edge penetrate deeper into the semiconductor bulk. Thus, the photogenerated minority carriers (holes in our cells) have a longer path to traverse to reach the liquid interface. If the thickness of the space charge layer substantially exceeds the absorption length, the minority carriers are swept practically instantaneously to the interface and oxidize the reducing ions of the solution. If, however, the thickness of the space charge layer is reduced by overdoping to substantially less than the absorption length,[1,5,6] carrier separation depends on diffusion. As long as the crystals and their surfaces are sufficiently perfect, the diffusion length exceeds the absorption length for all but the longest wavelengths absorbed and no substantial long-wavelength photocurrent defect is observed. This is obviously not the case with poorer crystals (which are technologically more realistic). In these, the diffusion length is shorter than the absorption length and a substantial long-wavelength defect exists in the photocurrent spectra. Since the absorbance usually increases at shorter wavelengths,[8] the defect gradually decreases at these. A corresponding gradual increase in photocurrent is noted not only in GaAs but also in other cells in which the semiconductor surface regions are imperfect. Examples include unetched CdS, CdSe, and CdTe cells (Figures 2-4), in which the polished surfaces have a high density of dislocations, extending 10^3-10^4 Å into the bulk.

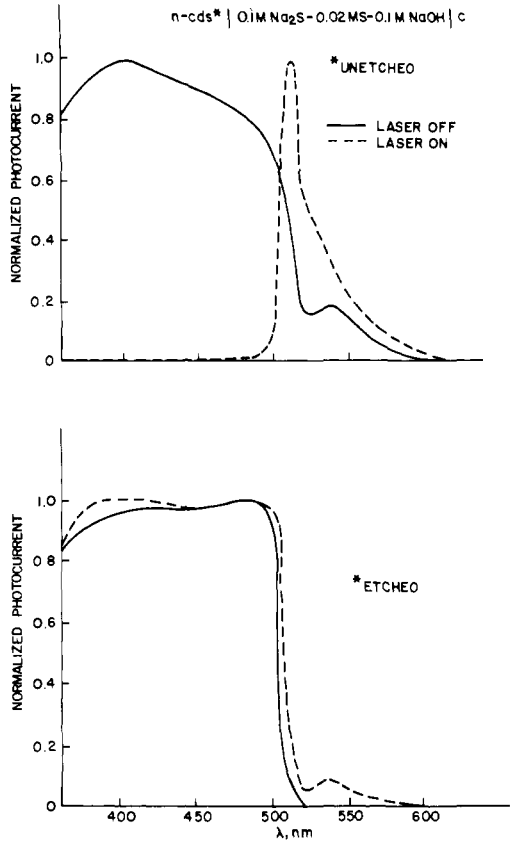

Figure 2. Photocurrent spectra of unetched and etched n-CdS|0.1 M Na_2S-0.02 M S-0.1 M NaOH|C cells. The solid lines show the spectra under low-level irradiance and the dashed lines under intense irradiance (Ar ion laser, 80 mW/cm^2).

Short-Wavelength Defects. Short-wavelength defects are characterized by a plateau or by a distinct maximum. These defects are more difficult to confirm experimentally in semiconductor liquid junction solar cells, since absorption by the solution may also reduce the short-wavelength response. An example of a short-wavelength defect is seen in Figure 2 (top) showing the photocurrent spectrum of the unetched n-CdS|0.1 M Na_2S-0.02 M S-0.1 M NaOH|C cell.

Short-wavelength defects in p-n junction solar cells are known to be due to surface recombination centers and to damage or impurities in the bulk very near the surface.[1] Short-wavelength light is absorbed predominantly in this region. As the absorption length decreases with decreasing wavelength, the density of carriers per unit volume, and thus the rate and probability of recombination, increases (if the density of recombination centers at or near the surface is substantial), since the density of minority carriers (and as will be seen later, if the band bending is substantial, also of majority carriers) near the interface also increases upon illumination. Wavelength defects due to surface and near-surface recombination centers can be distinguished from solution absorption losses by two-beam experiments in which one of the beams is used to increase the density of carriers near the surface, while normal photocurrent spectroscopy is done with the other. Contrary to absorption losses, which do not vary with light

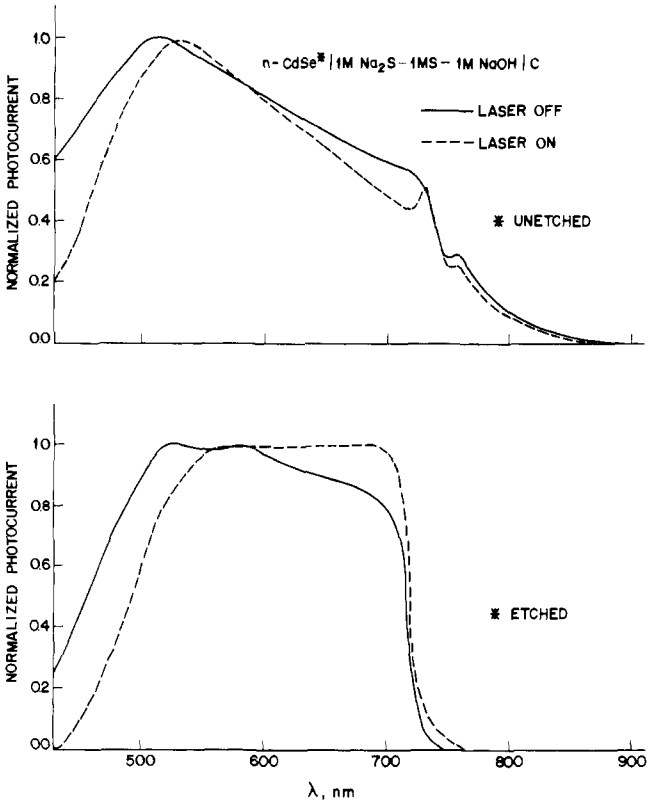

Figure 3. Photocurrent spectra of unetched and etched *n*-CdSe|1 M Na_2S-1 M S-1 M NaOH|C cells. The solid lines show the spectra under low-level irradiance and the dashed lines under intense irradiance (He-Ne laser, 60 mW/cm^2).

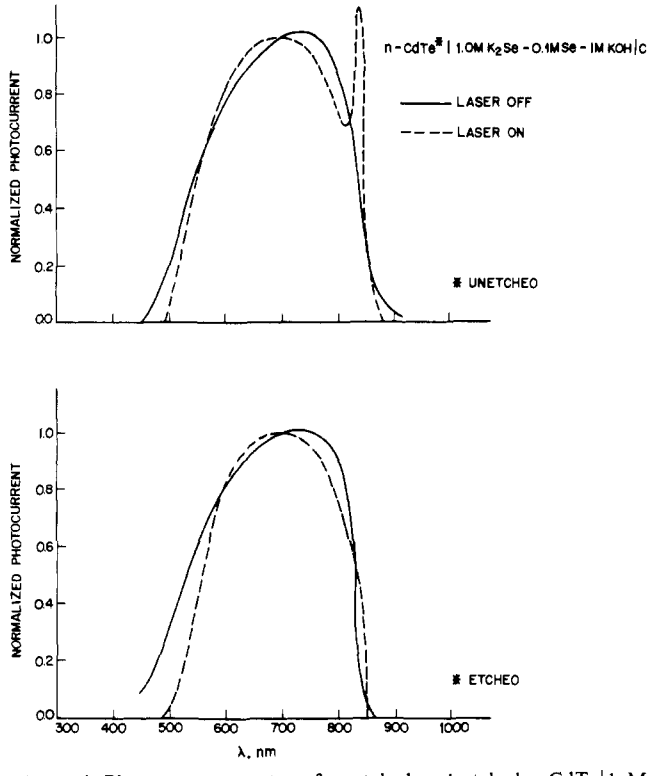

Figure 4. Photocurrent spectra of unetched and etched n-CdTe|1 M K_2Se-0.1 M Se-1 M KOH|C cells. The solid lines show the spectra under low-level irradiance and the dashed lines under intense irradiance (He-Ne laser, 60 mW/cm^2).

intensity, surface or near-surface recombination losses increase when the density of carriers is increased. The intensity dependence of the short-wavelength defect is overwhelming in the case of unetched CdS (Figure 2 top) and is observed also in CdSe cells (Figure 3) with both etched and unetched crystals.

Variations in Photocurrent Spectra with Irradiance. We find drastic changes in the photocurrent spectra of semiconductor liquid junction solar cells when the light intensity is increased.[5] The changes are minor when the surfaces of the semiconductors are well prepared, but are quite substantial when the semiconductor surfaces are of poor quality. Effects due to surface preparation may well account for the reported decrease in current efficiency with irradiance, even at modest light levels.

We interpret the irradiance dependence as being due to the presence of a high density of carrier recombination sites at or near the semiconductor-liquid interface. For example, dislocations near the surface introduced by cutting or polishing semiconductors act as recombination centers. Figures 2-4 show the irradiance dependence of spectra of cells with polished ("unetched") CdS, CdSe, and CdTe crystals and of cells from which the dense recombination center containing layer has been removed by etching. The intense irradiance ("laser on") experiments were run by flooding the crystals with a continuous laser beam, while measuring the modulated component of the photocurrent resulting from a chopped, weak, light beam from a monochromator, using phase sensitive detection.

The spectra of the cells with "unetched" crystals reveal transitions to or from states within the forbidden gap, which are enhanced when the irradiance is increased. Such a transition is not observable in the unetched n-CdTe|1 M K_2Se-0.1 M Se-1 M KOH|C cells (Figure 4, top) by classical photocurrent spectroscopy, but becomes the dominant feature in two-beam experiments. The enhancement of the transitions to or from states in the forbidden gap is not the only change taking place. As discussed earlier, short- or long-wavelength defects may be enhanced. In the case of the unetched CdS cell (Figure 2, top) increased irradiance effectively removes all but the longest wavelength components of the photocurrent spectrum. Measurement of the integrated quantum yields shows that the new spectrum is not due to enhancement of the response on the band edge side, but to a 50-fold reduction of the quantum yield at shorter wavelengths.

The light intensity dependent changes in the spectra are consistent with those expected for cells made with semiconductors having a high density of either electron or hole trapping states (Figures 5a and 5b). These states are populated by promotion ($h\nu_1$) of an electron from the valence band (VB) to the conduction band (CB) followed by carrier decay (A). The electron or hole trapping states (T) are separated from the conduction or valence bands, respectively, by nkT where n is a small number. The trapped electrons or holes are in thermal (Fermi-Dirac) equilibrium with the nearby bands, and may reenter these by thermal excitation (B). Thus, trapping impedes the motion of carriers in their respective bands, reducing their mobility and the rate of their separation, thus increasing their recombination probability. This results in a loss of photocurrent in all but two cases. First, there is no loss if the photogeneration takes place in a "perfect" zone of the semiconductor, in which the density of traps is inherently low. Second, there is no additional loss when the excitation is into or from a trapping state (Figures 5a and 5b). Photoexcitation into these states ($h\nu_2$) still leads to a photocurrent if the traps are sufficiently close to the respective bands, i.e., the traps are "shallow" and thermal excitation into these is probable. The above explains the fact that there is less loss in quantum yield for transitions into or from the forbidden gap and for transitions near the band gap energy than for transitions produced by shorter wavelengths.

Table I. Performance of Semiconductor Liquid Junction Solar Cells in Sunlight at an Irradiance near 75 mW/cm^2[a]

Cell	External conversion effic, %	Short circuit current density[a] mW/cm^2	Current effic, %	Open circuit voltage	Fill factor
n-CdS|0.1 M Na_2S-0.05 M S-0.1 M NaOH|C	1.3	4.0	80 ± 5	0.60	0.4
n-CdSe|1 M Na_2S-1 M S-1 M NaOH|C	8.4	14.0	80 ± 5	0.72	0.6
n-CdTe|1 M K_2Se-0.1 M Se-1 M KOH|C	8.4	18.1	70 ± 5	0.81	0.4
n-GaAs|1 M K_2Se-0.1 M Se-1 M KOH|C[9]	9.0	17.4	65 ± 5	0.65	0.6

[a] Measurements were performed at 69–77 mW/cm^2 of sunlight, then normalized to an irradiance of 75 mW/cm^2.

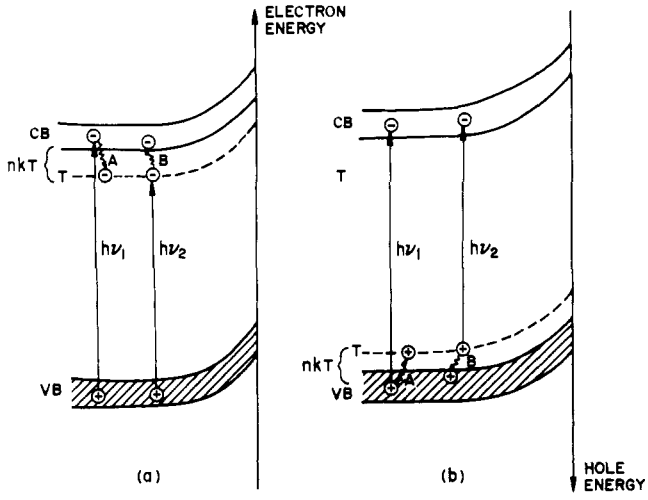

Figure 5. Trapping of electrons (a) and holes (b) near a semiconductor liquid interface. The liquid (not shown) is to the right of the drawings. VB, CB, and T denote the valence band, conduction band, and the trap, respectively. The trap is separated from the respective bands by an energy nkT, where n is small. A denotes processes of trapping and B processes of thermal excitation from the traps into the relevant bands. $h\nu_1$ denotes VB → CB transitions. $h\nu_2$ denotes VB → T transitions (a) or T → CB transitions (b).

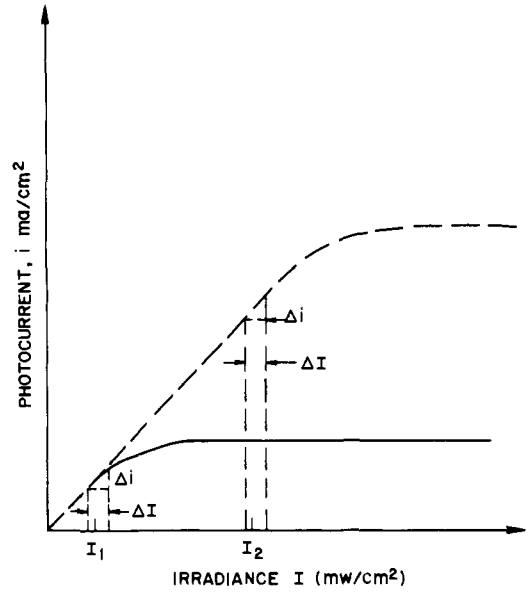

Figure 6. Photocurrent saturation at increased irradiance levels. The solid line represents a system in which the recombination rate is higher than that in a second, represented by a dashed line. At I_1 an increment in irradiance ΔI produces the same current increment Δi in both systems. At I_2 an increment ΔI in irradiance produces no photocurrent increment in the first system but continues to produce an increment Δi in the second.

The difference between the spectra of crystals with poor surfaces ("unetched") and with better surfaces ("etched") (Figures 2–4, top vs. bottom) is explained by the difference in the variation of the photocurrent yield as a function of irradiance in the two cases (Figure 6). In the case of a surface layer with a high density of traps, saturation sets in at a lower level of irradiance than in the case of a more perfect surface layer. The reason for this is that unless the majority and minority carriers are promptly separated, the rate of recombination increases linearly with the product of their concentrations and therefore, under circumstances to be defined, with the square of the irradiance. Furthermore, the concentration of at least one of the carriers increases with the density of traps. Saturation is reached when the incremental rate of photogeneration equals the incremental rate of recombination.

If the carriers are "promptly" separated, i.e., are separated within a period of time which is short relative to the period needed for their recombination, no saturation takes place. In any segment of semiconductor there is excess only of one of the carriers. As a result the rate of recombination is pseudo-first-order and, like the rate of photogeneration, varies linearly with irradiance. If, however, the carriers are not "promptly" separated, then at high levels of irradiance the concentrations of both carriers may increase with irradiance. Since the rate of recombination is proportional to the product of the concentrations, it may increase quadratically with irradiance, while the rate of photogeneration continues to increase only linearly. In this case the photocurrent does saturate.

Because of the high ($>10^{16}$ cm^{-3}) concentration of majority carriers in practical semiconductors, very high light intensities are needed to change the concentration of the majority carriers in the bulk. Thus, if the photons are absorbed in the bulk, where the concentration of the majority carriers is high, the rate of recombination will increase linearly with irradiance and no photocurrent saturation will take place at typical solar intensities. The situation at the proximity of the semiconductor liquid interface is, however, quite different. Because of the bending of the bands the majority carriers are depleted in this region. Consequently, photons absorbed in the depletion region, particularly near the liquid interface (where the depletion is most severe), may increase the concentrations of both majority and minority carriers. Consequently, the rate of their recombination increases with the square of the irradiance, causing saturation. The effect of a trap is, in this case, to increase the steady state concentration of one of the carriers by delaying it, or, stated differently, to prevent "prompt" carrier separation by the field associated with the depletion layer. It is significant that, if the thickness of the depletion region is sufficiently reduced by doping,[1,5,6] only the shorter wavelengths will be absorbed in the depletion region. In this case, the saturation and the resulting spectral defect are most pronounced at short wavelengths.

The above discussion defines some of the parameters that

affect the quality of a semiconductor in a liquid junction solar cell. Since "prompt" carrier separation is essential, and since carriers are separated more rapidly by the field associated with the depletion region than by mere diffusion, it is essential to exclude high concentrations of impurities which increase the concentration of the majority carrier and thus shrink the depletion layer to below the absorption length. Impurities which do not change the carrier concentration must be avoided only if they trap one of the carriers, substantially reducing its mobility. Thus, we believe that not all impurities in semiconductors are damaging to the performance of semiconductor liquid junction solar cells.

The "laser off" experiments of Figures 2–4 correspond to a level of irradiance, I_1 (Figure 6), at which there is no saturation. Consequently, a change in irradiance (ΔI) produces a similar change in current (Δi) in both the imperfect semiconductor with a high recombination rate and in the one with the better material having a low recombination rate. The photocurrent spectra of the unetched and etched materials are thus not greatly different. Once the irradiance is increased to I_2 ("laser on") a change in irradiance (ΔI) produces no change in the photocurrent (Δi) in the unetched material but continues to produce in the etched sample a current increment (Δi) identical with the earlier one. Consequently, the invariance of the photocurrent spectrum with irradiance at or above solar levels is an excellent indicator of the adequacy of the quality of a semiconductor in semiconductor liquid junction cell applications.

Using this criterion, we succeeded in attaining solar to electrical conversion efficiencies of 8–9% in several semiconductor liquid junction solar cells (Table I). The approximate short circuit current ("quantum") efficiencies range from 65 to 80% and would be closer to 100% if corrected for interface reflection and for solution absorption losses. Typical current–voltage curves for the unimproved ("unetched") and improved ("etched") CdSe cells are shown in Figure 7 of ref 7. At a typical solar irradiance (75 mW/cm^2) a 40-fold improvement in efficiency is observed between the two samples.

Experimental Section

The crystals used, the electrical contacts, the electrode structures, the auxiliary electrodes, the solutions, the light sources, the spectroscopic equipment, the electrochemical instrumentation, and the experimental method of measuring efficiencies are given in ref 7 except for the following. Cubic n-CdTe crystals cleaved in the (100) plane were purchased from Cleveland Crystals Inc., Cleveland, Ohio. The conductivities of the crystals were at least 0.1 Ω^{-1} cm^{-1}. Ohmic contacts were formed to the back of CdTe plates with indium amalgams. Sn and Si doped (100) and (111) cleaved GaAs crystals were used. The contacts to these were made with successively evaporated tin, palladium, and gold layers. The active crystal face was brought to 1 ± 0.5 mm of the window to minimize solution light absorption. In the CdTe and GaAs experiments the solution was 1 M K_2Se–0.1 M Se–1 M KOH. A 1-mm thick layer of this solution cuts off 50% of the light near 500 nm. CdTe crystals were etched for 30 s in a 1:1:1 solution of concentrated HCl, concentrated HNO_3, and saturated $K_2Cr_2O_7$. GaAs was etched in a 1:1:4 solution of 30% H_2O_2, water, and concentrated H_2SO_4 for 30 s. The initial spectra and voltammetric characteristics of all crystals as supplied could be changed by etching and restored by polishing with Linde A (0.3 μ alumina).

Acknowledgments. The authors wish to thank Howard Reiss and Bertram Schwartz for useful discussions.

References and Notes

(1) H. J. Hovel, "Semiconductors and Semimetals," Vol. 11, "Solar Cells", Academic Press, New York, N.Y., 1975, Chapter 2.
(2) H. Gerischer, *J. Electroanal. Chem.*, **58**, 263 (1975).
(3) A. B. Ellis, S. W. Kaiser, and M. S. Wrighton, *J. Am. Chem. Soc.*, **98**, 6855 (1976).
(4) A. B. Ellis, S. W. Kaiser, and M. S. Wrighton, *J. Am. Chem. Soc.*, **98**, 6419 (1976).
(5) B. Miller, A. Heller, M. Robbins, S. Menezes, K. C. Chang, and J. Thomson, Jr., *J. Electrochem. Soc.*, **124**, 1019 (1977).
(6) W. W. Anderson and Y. G. Chai, *Energy Convers.*, **15**, 85 (1976).
(7) A. Heller, K. C. Chang, and B. Miller, *J. Electrochem. Soc.*, **124**, 697 (1977).
(8) J. I. Pankove, "Optical Processes in Semiconductors", Prentice-Hall, Englewood Cliffs, N.J., 1971, Chapter 3.
(9) K. C. Chang, A. Heller, B. Schwartz, S. Menezes, and B. Miller, *Science*, **196**, 1097 (1977).

Anisotropic Motion inside a Micelle

F. M. Menger* and J. M. Jerkunica

Contribution from the Department of Chemistry, Emory University, Atlanta, Georgia 30322. *Received August 4, 1977*

Abstract: Carbon-13 spin–lattice relaxation times have been determined for monomeric and micellar ω-phenylalkanoic acids in aqueous base. Micellization decreases T_1's markedly for the aromatic carbons, e.g., T_1(para) = 2.9 and 0.39 for monomeric and micellar ω-phenyldecanoic acid, respectively. Moreover, micellization increases $R = T_1$(ortho)/T_1(para), a parameter indicative of anisotropic motion by the aromatic system. Thus, R = 3.6 for micellar ω-phenyldecanoate (compared, for example, with a value of only 1.8 for biphenyl). The results are interpreted in terms of an 11-fold faster rotation about the carbon–carbon bond linking the benzene ring with the chain relative to rotations about axes perpendicular to this bond. Diluting the phenyl-substituted surfactants with simple straight-chain surfactants (SDS and DTAB) does not suppress values of R significantly; hence, anisotropic motion within a micelle cannot be ascribed solely to phenyl/phenyl interactions. Anisotropic motion inside a micelle is shown to depend on the depth of the phenyl ring, the pH, and the presence of additives. A comparison of the micellar T_1 values with those in glycerol solutions of different viscosity demonstrates that the micelle interior is relatively fluid.

Problems of organization are intimately involved in living systems where thousands of reactions occur simultaneously. Because of the close relationship between life and molecular order, more and more attention is being focused on organized assemblages such as the micelle. Micelles and related aggregates provide information not available from the usual studies

0002-7863/78/1500-0688$01.00/0